NONLINEAR DYNAMIC MODEL FOR SEISMIC ANALYSIS OF NON-STRUCTURAL CLADDING

J. Hunt[1] and B. Stojadinovic[2]

[1] *Ph.D. Student, Department of Civil and Environmental Engineering, University of California, Berkeley, USA. Email: jphunt@berkeley.edu*

[2] *Professor, Department of Civil and Environmental Engineering, University of California, Berkeley, USA. Email: boza@ce.berkeley.edu*

ABSTRACT :

The seismic behavior of moment-frame structures with non-structural cladding in moderate to severe earthquakes has shown that the cladding panels and connections have a significant influence on the overall building response. However, analytical models that simulate the seismic response of structures with cladding have not been fully developed. In this paper we present a finite element model for nonlinear static and dynamic analyses of moment frame structures with cladding elements. These non-structural elements are attached to the structure using a small number of connectors intended to carry gravity loads, in-plane shear, and out-of-plane shear. The attachments are made using all-thread rods with double nuts or field fillet welds between angles, pipes, or plates embedded in non-structural panels and attached to the structure. In the proposed model, the panels are assumed to be rigid elements with a known mass. The attachments are modeled as multi-directional spring elements with cyclic force-deformation properties derived from attachment test data. The characteristics of the proposed model are examined in nonlinear static pushover and nonlinear dynamic time history analyses of the SAC Joint Venture 3-story building. The results show that the inclusion of cladding in the analytical model significantly affects the seismic response of the building.

KEYWORDS: analytical model, non-structural, cladding, seismic response

1. INTRODUCTION

Analytical and experimental studies have shown that exterior cladding panels have a major influence on structural behavior (Wolz et al., 1992; Henry et al., 1986; Goodno, 1983). However, in seismic analysis and design, engineers typically ignore the additional stiffness and damping that the cladding system may provide, which could prove to be beneficial or detrimental to the building's seismic performance. Depending upon the arrangement of the cladding panels and the connection types, the cladding provides increased lateral stiffness and strength to the supporting frame. Under linear dynamic analyses, the inclusion of cladding panels has been shown to decrease the interstory drifts and increase forces in the supporting frame members (Goodno, 1983). However, there have been few nonlinear analytical studies on the effect of cladding on the overall seismic behavior of a building.

In this paper, the authors present a two-dimensional analytical model to investigate the effect of non-structural cladding on the seismic response of the three-story SAC building. Rigid beam-column elements were used to model the cladding panels, and nonlinear spring elements were used to model the cladding connections. A modal analysis, nonlinear static pushover analysis, and nonlinear dynamic time history analyses were performed for the bare frame model and the model with cladding. The inclusion of cladding significantly modified the response of the building: the first three fundamental periods decreased by 26%, 18%, and 6%, respectively. The pushover curve revealed that the initial lateral stiffness of the model with cladding is approximately twice as stiff as the initial lateral stiffness of the bare frame model, and the post yield strength of the model with cladding at 4% roof drift is 55% higher than the post yield strength of the bare frame model. The results of the dynamic time history analyses show that the cladding panels affect both the lateral drift and base shear response.

2. ANALYTICAL MODEL OF 3-STORY SAC BUILDING

The three-story SAC building (Foutch, 2000) was selected as the study building in which to apply cladding panels, and a two-dimensional nonlinear model was created in Opensees (McKenna et al., 2000). Two analytical models were considered: (1) a bare frame model consisting of moment-resisting and gravity framing and (2) the bare frame model with cladding panels and connections. An elevation of the model with cladding panels is shown in Figure 1. The beams and columns of the moment resisting frame are modeled with nonlinear force beam-column elements capable of capturing distributed plasticity using five integration points along each element. The wide-flange sections were modeled using fiber sections consisting of three rectangles with several "layers" or fibers to capture changes in the stress-strain through the section. The fiber response is integrated across the section to provide resultant section forces at each integration point. The steel material stress-strain relationship is predefined with the Giuffre-Menegotto-Pinto model. The yield stress was selected as 50 ksi, and the modulus of elasticity was selected as 29,000 ksi for all elements. The strain-hardening ratio (ratio between post-yield tangent and initial elastic tangent) was selected as 2%. The beams of the gravity framing are modeled with elastic beam column elements. The concrete floor slab was modeled using rigid diaphragm constraints, and the seismic mass was represented as lumped masses at the nodes. In Figure 1, the moment frames are shown as thick dotted lines, and the gravity frames are shown as thin dotted lines.

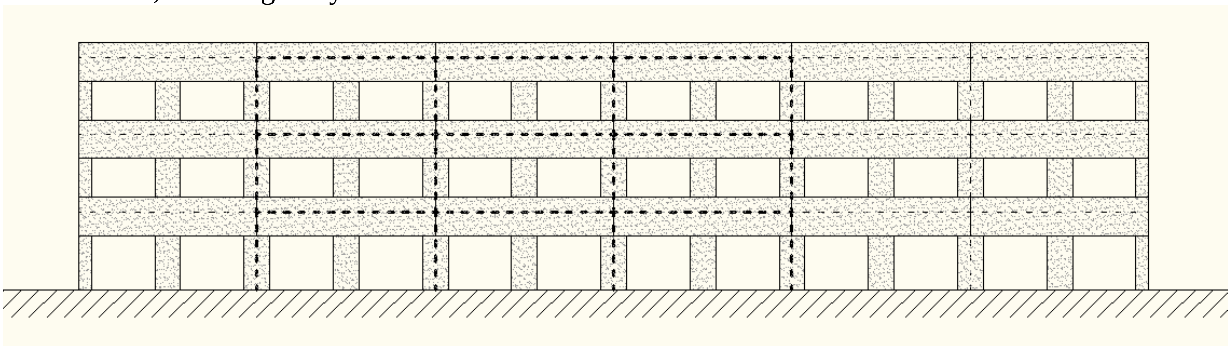

Figure 1 Exterior framing and cladding of 3-story SAC building (east-west direction)

The model with cladding uses the same bare frame as described above. The cladding system is made up of individual spandrel (beam) panels and column covers, as shown in Figure 1.

2.1. Cladding Panels

The cladding panels were assumed to be rigid (Wolz et al., 1992; Goodno et al., 1991) and were represented with rigid frame elements. The cladding system is made up of spandrel panels (covering the beams), and intermediate column panels (covering the columns), as shown in Figure 2. The spandrel panels are 30 feet wide by 6.5 feet tall by 5 inches thick, and the column panels are 4.25 feet wide by 6.5 feet tall by 5 inches thick.

The different types and arrangements of the cladding connections are shown in Figure 2a. The cladding connections are modeled as zero-length "spring" elements in Opensees, and the force deformation relationship is prescribed for each connection in three directions (horizontal direction, vertical direction, and rotation). The spandrel panels are connected at their corners to the columns with push-pull connections that transmit shear forces between the cladding and frame by bending of a threaded rod. The middle of the spandrel panels are connected to the beams with rigid lateral connections (rigid plates) that prevent relative horizontal displacement between the spandrel panel and the supporting beam. There are two vertical bearing connections in the spandrel panels that provide a rigid connection in compression but no tension or lateral force resistance. The column covers span the gap between the spandrel panels, and they are attached to the spandrel panels with two slotted connections at their tops and two pinned connections at their bottoms. An exploded view of the connections between the cladding system and the supporting framing is shown in Figure 2b. In addition, the cladding panel masses are assigned to the corners of each panel: 0.008 kips*sec^2/in at the corners of the spandrel panels and 0.001 kips*sec^2/in at the corners of the column covers. The lumped masses at the nodes in the gravity and moment-resisting frames are decreased so that the total seismic mass in the model with cladding is the same as the total seismic mass in the bare frame model.

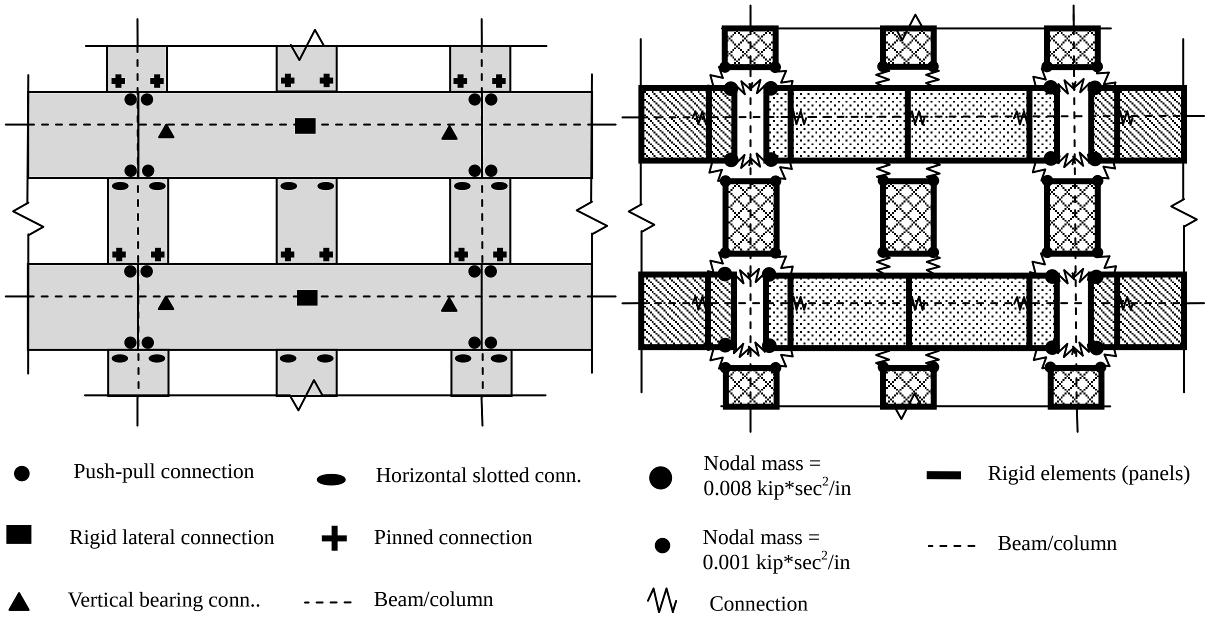

(a) cladding system and connections *(b) cladding system model (exploded view)*

Figure 2 Cladding system and connections

2.2. Cladding Panel Connections

As shown in Figure 2, the cladding panels are attached to the framing with push-pull connections, rigid lateral connections, vertical bearing connections, slotted connections, and pinned connections. The push-pull connections are used to join the corners of the spandrel panels to the columns, and the shear force-deformation values were taken from McMullin et al. (2004). The modeled shear force-deformation relationship is shown in Figure 3a. Due to the slender aspect ratio of the threaded rod, the moment-rotation behavior is neglected.

The rigid lateral connection is used to attach the middle of the panel to the supporting beam at midspan. The connection consists of a wide flat plate that deforms in shear. The lateral resistance of the plate is sufficiently large enough that the connection is idealized as essentially rigid (large shear stiffness is assigned).

The vertical bearing connections are used to provide gravity support to the spandrel panel. Each spandrel panel is supported vertically at two locations near the ends of the supporting beams. The bearing connection consists of a leveling bolt that rests on the beam slab and is welded to an embed in the spandrel panel. Therefore, the vertical bearing connection can only resist compression force. The compression force-deformation relationship of the leveling bolt bearing on the concrete slab is essentially rigid, as shown in Figure 3b.

The column covers and intermediate panels are connected directly to the neighboring spandrel panels instead of the supporting framing. The bottom of the column covers are pin connected to the top of the spandrel panels, providing stiffness in the horizontal and vertical shear directions but no moment resistance. The shear force-deformation relationship is represented with the nonlinear model shown in Figure 3c. The tops of the column covers are connected to the bottom of the spandrel panels with bolted-slotted connections. The shear force-deformation relationship of the slotted connections is defined with a hysteretic material, shown in Figure 3d, that captures the binding and failure of the connections.

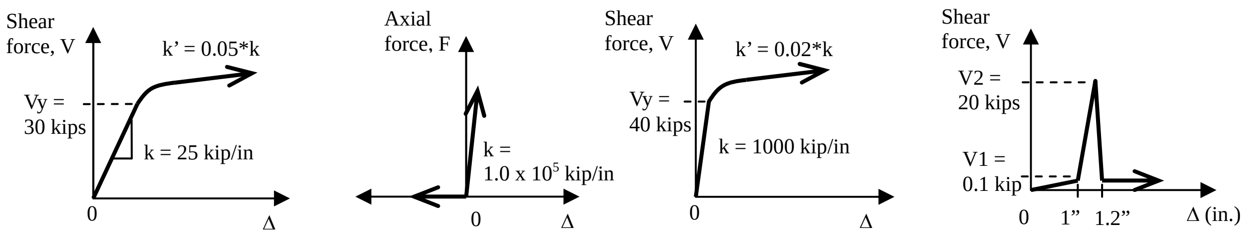

(a) push-pull connection (b) bearing connection (c) column cover pinned connection (d) column cover slotted connection

Figure 3 Force-deformation relationships for cladding panel connections

3. NONLINEAR ANALYSES OF 3-STORY SAC BUILDING

The seismic response of the bare frame model and the model with cladding are compared by examining the results of modal analyses, nonlinear static pushover analyses, and dynamic time history analyses.

3.1. Modal Analysis

The total seismic mass is the same for the bare frame model and the model with cladding. A modal analysis was performed to investigate the effect of the addition of cladding to the free vibration properties of the structure. The first three modal periods are given below in Table 1.

Table 1 Comparison of modal periods

Model	Modal Period (sec.)		
	Mode 1	Mode 2	Mode 3
Bare frame model	1.045	0.322	0.167
Model with cladding	0.774	0.264	0.157

When cladding is included, the first three fundamental periods decreased by 26%, 18%, and 6%, respectively. The shapes of the first three modes are shown in Figure 4. The first mode shape of the bare frame model is approximately linear, while the first mode shape of the model with cladding shows a possible soft-story mechanism in the first story. The second and third mode shapes also reveal differences in the modal ordinates between the two models.

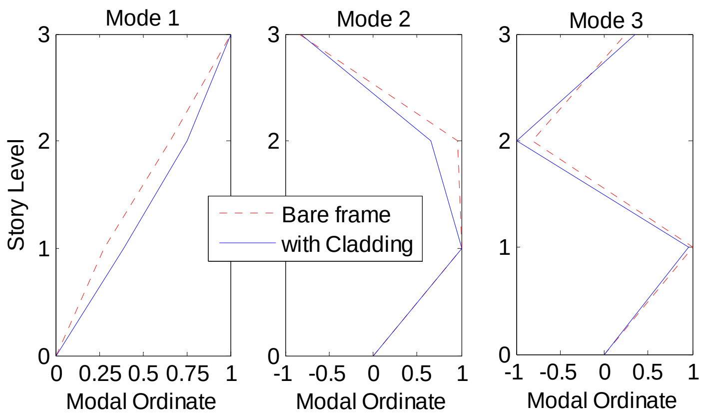

Figure 4 Comparison of mode shapes

3.2. Pushover Analysis

A static nonlinear pushover analysis was performed for the bare frame model and the model with cladding. The pushover analyses were started after first applying the gravity loads, and the co-rotational geometric transformation was used to account for second-order P-Delta effects. The applied force distribution was proportional to the first mode shapes (approximately linear), and a displacement controlled algorithm was used to monitor the roof displacement and calculate the applied load factor. As shown in Figure 5a, the pushover analyses were continued to an average roof drift angle of 6.4%.

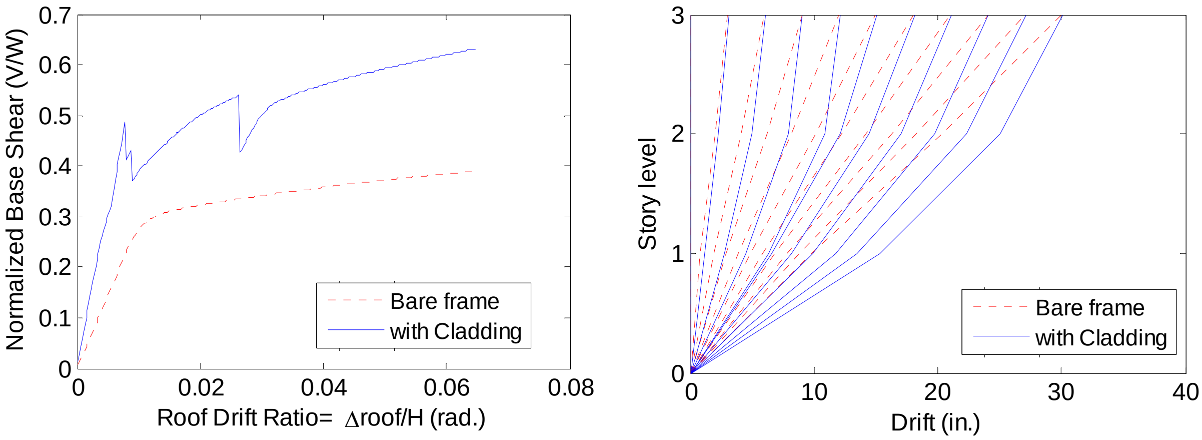

(a) Pushover curve

(b) Deflected shape at selected drift levels

Figure 5 Comparison of pushover curves and deflected shapes

For the model with cladding, the initial lateral stiffness is approximately twice the initial lateral stiffness of the bare frame model, and the post yield strength of the model with cladding at 4% roof drift is 55% higher than the post yield strength of the bare frame model. As the model with cladding deforms laterally, the binding action of the slotted connections causes the increased stiffness. Then, the slotted connections in the interior column covers fail at 1% roof drift, and the slotted connections in the exterior column covers fail at 2.5% drift. As shown in Figure 5b, the deflected shape of the bare frame model remains approximately linear throughout the pushover analysis. However, the model with cladding develops a soft-story mechanism in the first story when the roof drift exceeds 5 inches.

3.3. Time History Analysis

Time-history analyses were performed to evaluate the nonlinear dynamic response of the frames to moderate and severe ground motions. Seven ground motions were selected that are representative of a site near the UC Berkeley campus in California. The ground motions were scaled to an intensity corresponding to the Life Safety performance level with 10% in 50 year probability of exceedance and the Collapse Prevention performance with 2% in 50 year probability of exceedance, as described by FEMA 356. The ground motions were scaled so that their spectral acceleration at the first modal period of the frame matched the spectral acceleration of the design spectrum at the first modal period. The scale factors varied between 0.3 and 3.0. The time-history analyses were performed with the Newmark integration scheme and 4% Rayleigh damping for the first three modes.

The roof displacements computed during the time-history analyses for three of the seven ground motions are shown in Figure 6. The plots are shown for the 2% in 50 year hazard level. For the EZerzi ground motion, the roof displacements of the model with cladding are similar to the roof displacements of the bare frame model. At the first displacement peak at 3 seconds, the response of the model with cladding is smaller than the response of the bare frame model. However, at the next peak at 4 seconds, the response of the model with cladding is slightly larger than the response of the bare frame model. For the LPlgpc motion, the roof displacements of the model with cladding are significantly smaller than the roof displacements of the bare frame model. The bare frame model undergoes residual displacements after 12 seconds which are never recovered, while the model with cladding shows no residual displacements. Finally, for the TOhino motion, the roof displacements of the model with cladding are smaller than the roof displacements of the bare frame model. The response of the model with cladding also shows no residual displacements for this ground motion.

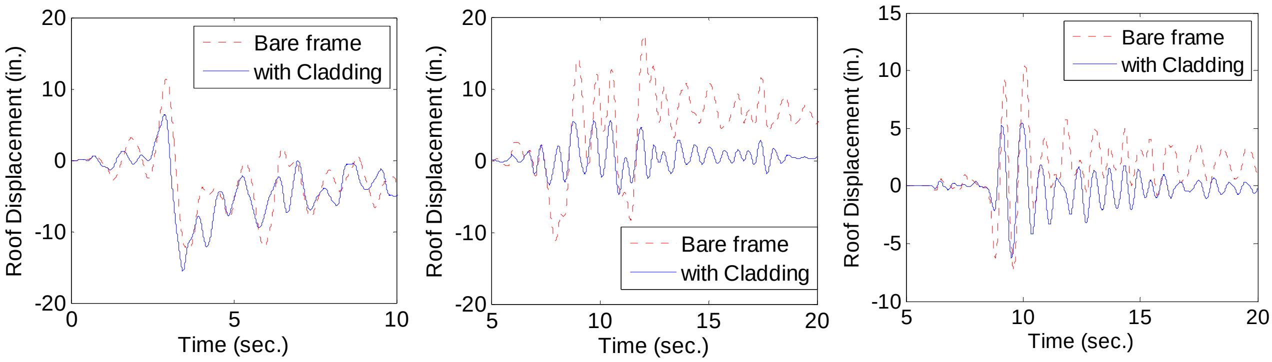

(a) EZerzi motion *(b) LPlgpc motion* *(c) TOhino motion*

Figure 6 Time-history of roof displacements for 2%/50 yr. hazard level (selected ground motions)

The maximum roof displacements of both models for all seven ground motions corresponding to the 10% in 50 year and 2% in 50 year hazard levels are plotted in Figure 7. The median maximum roof displacements and standard deviations are also shown. For the 10% in 50 year hazard level, the median maximum roof displacement of the model with cladding is 6.0 inches, and the median maximum roof displacement of the bare frame model is 9.2 inches. For the 2% in 50 year hazard level, the median maximum roof displacement of the model with cladding is 9.4 inches, and the median maximum roof displacement of the bare frame model is 13.2 inches. The differences between the displacements of the lower stories are less significant between the two models, due to the first-story mechanism that develops in the model with cladding.

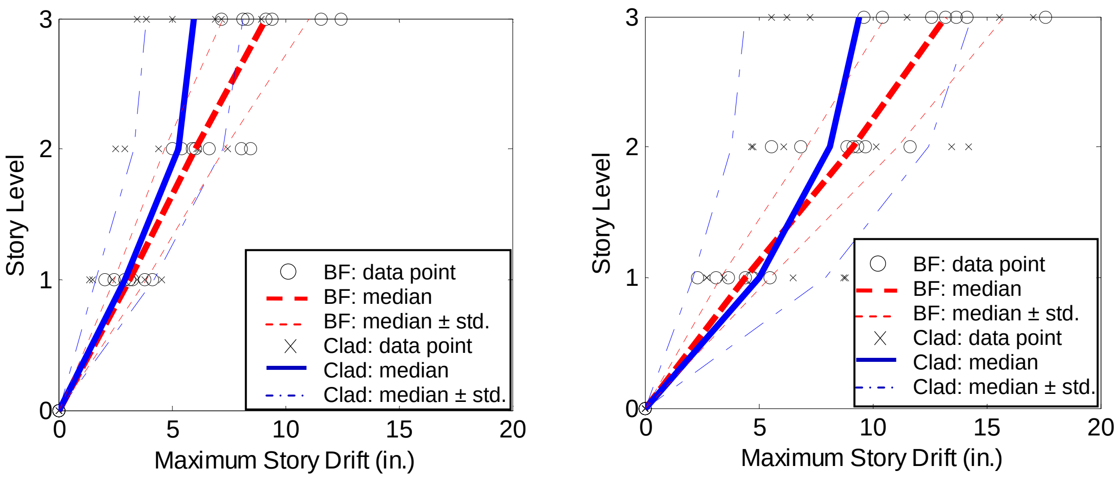

(a) 10% in 50 years *(b) 2% in 50 years*

Figure 7 Median maximum story displacements for two hazard levels (BF = bare frame, Clad = with Cladding)

The time-history of the base shear versus first-story displacement of one of the first-story interior columns in the moment frame was recorded for the EZerzi and LPlgpc ground motions corresponding to the 2% in 50 year hazard level. The results for the bare frame model and the model with cladding are shown in Figure 8. For the

EZerzi motion, the response of an interior column in the model with cladding shows larger shear forces and much larger displacements than the base shear and displacements in the bare frame model. On the other hand, the response of an interior column during the LPlgpc motion shows that the first-story displacement in the model with cladding is much smaller than the first-story displacement in the bare frame model. The maximum base shear forces in an interior column are approximately the same between the two models.

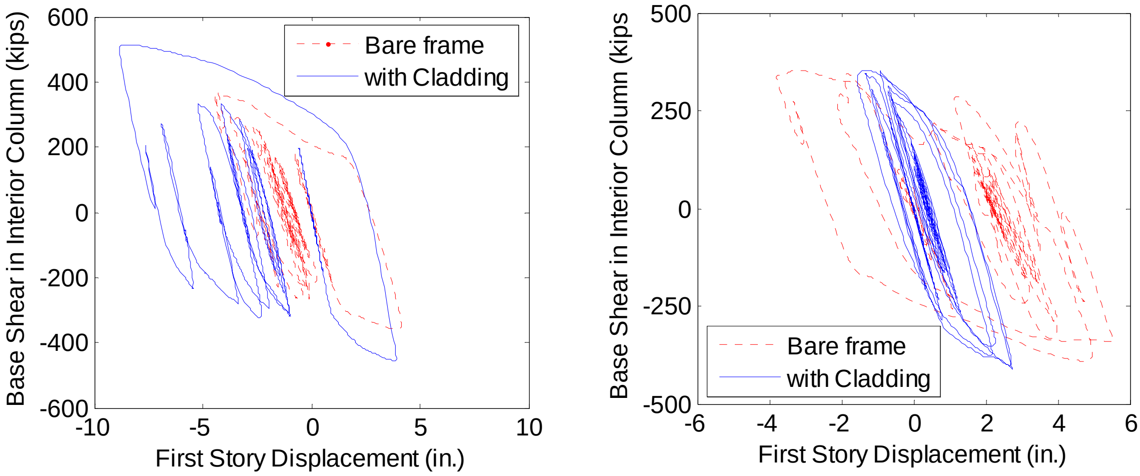

(a) EZerzi motion, 2% in 50 year *(b) LPlgpc motion, 2% in 50 year*

Figure 8 Base shear versus first story displacement of an interior column (2% in 50 year hazard level)

The dynamic time-history analyses reveal that the addition of the cladding system to the analytical model may have a beneficial effect (decreased story displacements or no residual displacements) or a detrimental effect (increased story displacements or increased base shear forces). The cladding system may also cause an undesirable first-story collapse mechanism.

4. CONCLUSIONS

A two-dimensional analytical model of the 3-story SAC building was created in Opensees to investigate the effect of nonstructural cladding on the seismic response of the supporting frame. The cladding panels were modeled as rigid frame elements, and the cladding-to-frame connections were idealized with zero-length nonlinear spring elements. A modal analysis, nonlinear static pushover analysis, and nonlinear dynamic time history analyses were performed for the bare frame mode and the model with cladding. The first three fundamental periods decreased by 26%, 18%, and 6%, respectively, with the addition of the cladding system. The pushover curve revealed that the initial lateral stiffness of the model with cladding is both stiffer and stronger than the bare frame model. The models were also subjected to time-history analyses for hazard levels of 10% in 50 years and 2% in 50 years. The median roof displacement response of the model with cladding was smaller than the median roof displacement response of the bare frame model. The time histories of the base shear versus first-story displacement of an interior column revealed that the addition of cladding may be either beneficial or detrimental, depending on the ground motion. This study shows that the contribution of the cladding system to the lateral stiffness and the dynamic response of the building should not be ignored.

ACKNOWLEDGEMENTS

This data is based upon work supported by the National Science Foundation under the project NEESR-SG: Experimental Determination of Performance of Drift-Sensitive Nonstructural Systems under Seismic Loading, CMS-0619157. This support is gratefully acknowledged. Any opinions, findings, and conclusions or recommendations expressed in this material are those of the authors and do not necessarily reflect the views of the National Science Foundation.

REFERENCES

FEMA 350 (2000). Recommended Seismic Design Criteria for New Steel Moment-Frame Buildings, *Report No. FEMA 350*, Federal Emergency Management Agency, Washington, DC.

Foutch, D.A. 2000. State of the Art Report on Performance Prediction and Evaluation of Steel Moment-Frame Buildings. *SAC Report No. FEMA 355F*. Federal Emergency Management Agency. Washington, D.C.

Goodno, B. J. (1983). Cladding-Structure Interaction in Highrise Buildings, Schools of Civil and Aerospace Engineering, Georgia Institute of Technology, 2 Vols.

Goodno, B. J., Craig, J., and Hsu, C. C. (1991). Experimental Studies and Analytical Evaluation of Ductile Cladding Connections, Proc*eedings of the Pacific Conference on Earthquake Engineering*, New Zealand, November 20-23, pp. 43-54.

Henry, R. M. and Roll, F. (1986). Cladding-Frame Interaction, *Journal of Structural Engineering*, **Vol. 112, No. 4**, April, pp. 815-834.

McKenna, F., Fenves, G.L., Scott, M.H., and Jeremic, B. (2000). Open system for earthquake engineering simulation. Web page: http://OpenSees.berkeley.edu.

McMullin, K., Wong, Y., Choi, C., Chan, K. (2004). Seismic Performance States of Precast Concrete Cladding Connections, *Proceedings of 13th World Conference on Earthquake Engineering*, Vancouver, B.C., Canada, August 1-6, Paper No. 3379.

Wolz, M., Hsu, C. C., and Goodno, B. J. (1992). Nonlinear Interaction between Building Structural Systems and Nonstructural Cladding Components, *Proceedings of ATC-29 Seminar and Workshop on Seismic Design and Performance of Equipment and Nonstructural Elements in Buildings and Industrial Structures*, pp. 329-340.